Journal of Inorganic Biochemistry 214 (2021) 111272

Contents lists available at ScienceDirect

Journal of Inorganic Biochemistry

journal homepage: www.elsevier.com/locate/jinorgbio

Short Communication

Kinetic inequivalence between α and β subunits of ligand dissociation from ferrous nitrosylated human haptoglobin:hemoglobin complexes. A comparison with O_2 and CO dissociation

Paolo Ascenzi [a,*], Giovanna De Simone [b], Andrea Pasquadibisceglie [b], Magda Gioia [c,d], Massimo Coletta [c,d]

[a] Interdepartmental Laboratory for Electron Microscopy, Roma Tre University, Via della Vasca Navale 79, I-00146 Roma, Italy
[b] Department of Sciences, Roma Tre University, Viale Guglielmo Marconi 79, I-00146 Roma, Italy
[c] Department of Clinical Sciences and Translational Medicine, University of Roma "Tor Vergata", Via Montpellier 1, I-00133 Roma, Italy
[d] Interuniversity Consortium for the Research on the Chemistry of Metals in Biological Systems, Via Celso Ulpiani 27, I-70126, Bari, Italy

ARTICLE INFO

Keywords:
Human haptoglobin 1–1:hemoglobin complex
Human haptoglobin 2–2:hemoglobin complex
Nitrogen Monoxide Dissociation
Kinetics

ABSTRACT

Haptoglobin (Hp) counterbalances the adverse effects of extra-erythrocytic hemoglobin (Hb) by trapping the αβ dimers of Hb in the bloodstream. In turn, the Hp:Hb complexes display Hb-like reactivity. Here, the kinetics of NO dissociation from ferrous nitrosylated Hp:Hb complexes (*i.e.*, Hp1–1:Hb(II)-NO and Hp2–2:Hb(II)-NO, respectively) are reported at pH 7.0 and 20.0 °C. NO dissociation from Hp:Hb(II)-NO complexes has been followed by replacing NO with CO. Denitrosylation kinetics of Hp1–1:Hb(II)-NO and Hp2–2:Hb(II)-NO are biphasic, the relative amplitude of the fast and slow phase being 0.495 ± 0.015 and 0.485 ± 0.025, respectively. Values of $k_{off(NO)1}$ and $k_{off(NO)2}$ (*i.e.*, (6.4 ± 0.8) × 10^{-5} s^{-1} and (3.6 ± 0.6) × 10^{-5} s^{-1} for Hp1–1:Hb(II)-NO and (5.8 ± 0.8) × 10^{-5} s^{-1} and (3.1 ± 0.6) × 10^{-5} s^{-1} for Hp2–2:Hb(II)-NO) are unaffected by allosteric effectors and correspond to those reported for the α and β subunits of tetrameric Hb(II)-NO and isolated α(II)-NO and β(II)-NO chains, respectively. This highlights the view that the conformation of the Hb $\alpha_1\beta_1$ and $\alpha_2\beta_2$ dimers matches that of the Hb high affinity conformation. Moreover, the observed functional heterogeneity reflects the variation of energy barriers for the ligand detachment and exit pathway(s) associated to the different structural arrangement of the two subunits in the nitrosylated R-state. Noteworthy, the extent of the inequivalence of α and β chains is closely similar for the O_2, NO and CO dissociation in the R-state, suggesting that it is solely determined by the structural difference between the two subunits.

1. Introduction

Haptoglobin (Hp) is a chaperone-like molecule, which binds αβ dimers of plasma Hb, bringing about the formation of a very stable non-covalent complex, which prevents most harmful effects related to the presence of free Hb and/or free heme in the bloodstream, such as (*i*) heme dissociation from Hb, and (*ii*) heme oxidation, facilitating the removal of Hb *via* the reticuloendothelial system and the CD163 receptor-mediated endocytosis by hepatocytes, Kupffer cells, and tissue macrophages [1–8]. Further, Hp binding to αβHb dimers prevents hydrogen-peroxide radical formation and migration, subunit dissociation, globin-cross linking, and heme release, thereby protecting the vascular system from damage by free Hb [8,9].

From a molecular viewpoint, $\alpha_1\beta_1$ (and $\alpha_2\beta_2$) dimers (*i.e.*, the products of the tetramer to dimer dissociation of human hemoglobin; Hb) have been always considered to be locked in the high-affinity R conformation (with no "heme-heme" interactions and no Bohr effect) [8,10–23]. Therefore, ligand binding properties of Hb dimers bound to haptoglobin (Hp) represent an excellent molecular model to study the functional features of pure dimeric species without the interference of

Abbreviations: BZF, bezafibrate; Hb, human hemoglobin; Hb(III), ferric Hb; Hb(II), ferrous Hb; Hb(II)-O_2, oxygenated Hb(II); Hb(II)-CO, carbonylated Hb(II); Hb(II)-NO, nitrosylated Hb(II); Hp, human haptoglobin; Hp1–1, phenotype 1–1 of Hp; Hp1–1:Hb(III), ferric Hp1–1:Hb complex; Hp1–1:Hb(II), ferrous Hp1–1:Hb complex; Hp2–2, phenotype 2–2 of Hp; Hp2–2:Hb(III), ferric Hp 2–2:Hb complex; Hp2–2:Hb(II), ferrous Hp 2–2:Hb complex; IHP, D-myo-inositol 1,2,3,4,5,6-hexakisphosphate; Mb, myoglobin.

* Corresponding author.
E-mail address: ascenzi@uniroma3.it (P. Ascenzi).

https://doi.org/10.1016/j.jinorgbio.2020.111272
Received 24 February 2020; Received in revised form 4 October 2020; Accepted 4 October 2020
Available online 16 October 2020

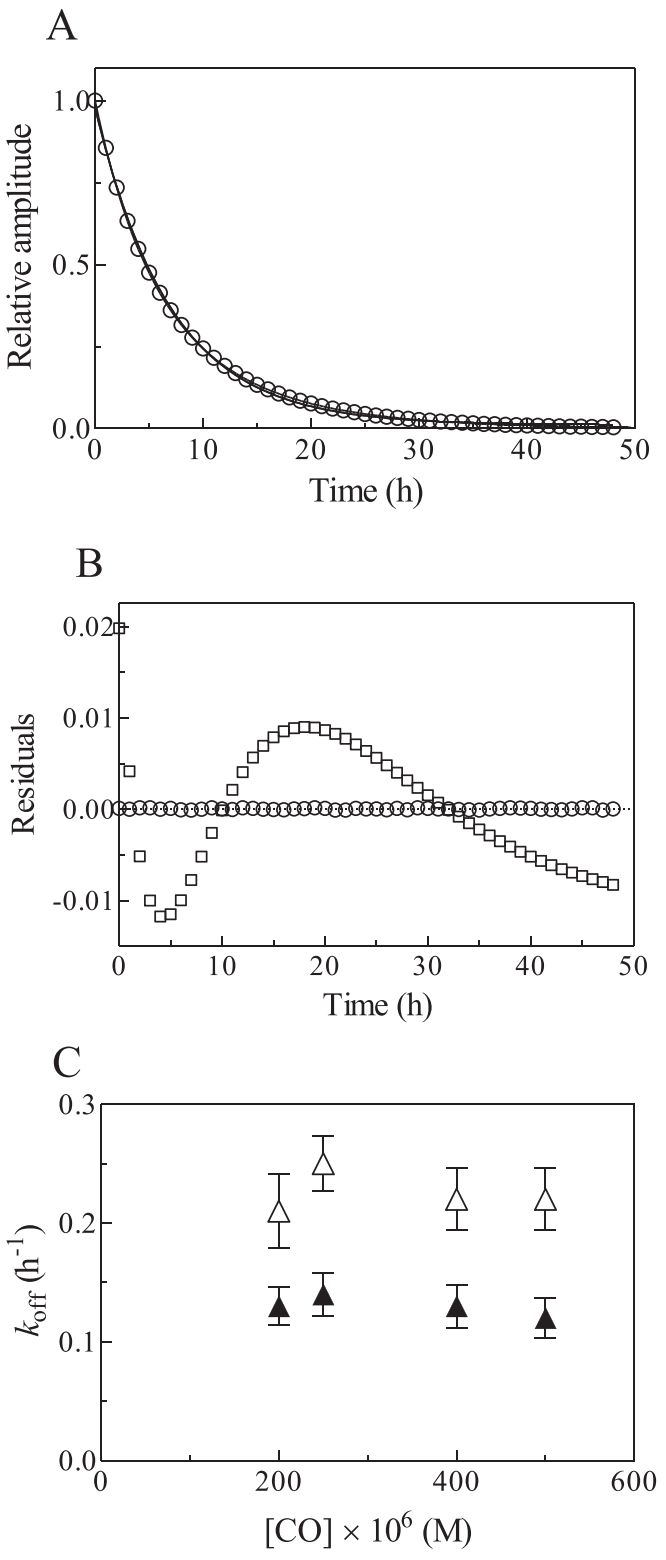

(caption on next column)

Fig. 1. Kinetics of NO dissociation from Hp1–1:Hb(II)-NO, at pH 7.0 and 20.0 °C. (A) Time course of NO dissociation from Hp1–1:Hb(II)-NO. The CO concentration was 5.0×10^{-4} M. The time course analysis according to eq. (1) allowed to determine the values of $k_{off(NO)1} = 2.2 \times 10^{-1}$ h^{-1} (= 6.1×10^{-5} s^{-1}), $A_1 = 0.48$, $k_{off(NO)2} = 1.2 \times 10^{-1}$ h^{-1} (= 3.3×10^{-5} s^{-1}), and $A_2 = 0.52$. The time course analysis according to eq. (2) allowed to determine the values of $k_{off\ (NO)} = 1.4 \times 10^{-1}$ h^{-1} (= 3.9×10^{-5} s^{-1}) and $A = 1.0$. (B) Residuals obtained from the non-linear least-squares fitting with one (squares; eq. (2)) and two (circles; eq. (1)) exponential(s) of data referring to NO dissociation from Hp1–1:Hb(II)-NO. (C) Dependence of the first order rate constant for NO dissociation from Hp1–1:Hb(II)-NO on the CO concentration. The average values of $k_{off(NO)1}$ and $k_{off(NO)2}$ are 2.3×10^{-1} h^{-1} (= 6.4×10^{-5} s^{-1}) and 1.3×10^{-1} h^{-1} (= 3.6×10^{-5} s^{-1}), respectively. The Hp1–1:Hb(II)-NO concentration was 4.8×10^{-6} M. The dithionite concentration was 2.0×10^{-3} M.

the tetrameric population, which is present to a relevant extent even at the lowest affordable concentrations (*i.e.*, 5.0×10^{-7} to 1.0×10^{-6} M) in the *in vitro* experiments [24].

We have recently characterized the functional properties of ferrous and ferric Hp:Hb complexes, putting in evidence a marked subunit functional heterogeneity for most of the ligands investigated (namely O_2 and CO for the ferrous form and azide, thiocyanate and imidazole for the ferric form) [8,23,25–27]. However, only in the ferric form we have observed an assembly-linked structural change of ferric Hb upon dimer association to tetramer, as indicated by a much faster dissociation of the sixth axial ligand H_2O from ferric hemes in Hp:Hb complexes (as well as in isolated subunits) with respect to the tetramer [26,28].

Kinetics of the reductive nitrosylation of ferric human haptoglobin1–1: and haptoglobin2–2:hemoglobin complexes (Hp1–1: Hb(III) and Hp2–2:Hb(III), respectively) [21] allowed: (*i*) to estimate the values of the lowest limits of the second-order rate constant for Hp1–1: Hb(III) and Hp2–2:Hb(III) nitrosylation (*i.e.*, $k_{on} \geq 3.8 \times 10^6$ M^{-1} s^{-1}, since at the NO concentrations employed it was too fast to be observed by rapid-mixing stopped-flow technique) and of the first-order rate constant for Hp1–1:Hb(III)- NO and Hp2–2:Hb(III)-NO denitrosylation (*i.e.*, $k_{off} \geq 4.4 \times 10^2$ s^{-1}), and (*ii*) to determine the values of the second-order rate constant for the nitrosylation of ferrous human haptoglobin1–1: and haptoglobin2–2:hemoglobin complexes (Hp1–1: Hb(II) and Hp2–2:Hb(II); *i.e.*, 1.1×10^7 M^{-1} s^{-1} and 9.3×10^6 M^{-1} s^{-1}, respectively). Of note, kinetic parameters for (de)nitrosylation of Hp:Hb (III)(-NO) and Hp:Hb(II)(-NO) complexes agree with those reported for horse heart myoglobin (Mb), sperm whale Mb, and human Hb [29–31].

Differently from O_2 and CO, values of the second-order rate constants for the nitrosylation of the T- and R-states Hb(II) are rather similar, indicating that the cooperativity for NO binding to Hb(II) is exclusively expressed on the ligand dissociation [15,30,32–34]. Therefore, only the determination of the NO dissociation rate constants allows a clear identification of the quaternary conformation of Hp1–1:Hb(II)-NO and Hp2–2:Hb(II)-NO. Here, kinetics of NO dissociation from Hp1–1:Hb(II)-NO and Hp2–2:Hb(II)-NO by CO replacement are reported, highlighting the view that the conformation of the ferrous nitrosylated αβ dimers bound to Hp1–1 and Hp2–2 matches that of the R-state of the Hb tetramer and of isolated α and β subunits.

2. Materials

Human Hp1–1 and Hp2–2 were purchased from Athens Research & Technology, Inc. (Athens, GA, USA) and Merck KGaA (Darmstadt, Germany). Oxygenated human Hb (Hb(II)-O_2) was prepared as previously reported [15]. The Hp:Hb complexes were prepared by mixing Hb(II)-O_2 with Hp1–1 and Hp2–2 at pH 7.0 and 20.0 °C [11,12,16,22]. Each Hp dimer binds one or two αβ dimers of Hb. To avoid the occurrence of free Hb an excess of Hp1–1 and Hp2–2 (from 20 to 100%) was present in all samples and the absence of free Hb was checked by gel electrophoresis (Fig. 1 SM of Supplementary Material) [12,35–37]. Hp1–1:Hb(II)-NO and Hp2–2:Hb(II)-NO (final concentration 4.8×10^{-6} M and 4.6×10^{-6}

$$\text{Hp:Hb(II)-NO} + \text{CO} \underset{k_{on(NO)}}{\overset{k_{off(NO)}}{\rightleftharpoons}} \text{Hp:Hb(II)} + \text{NO} + \text{CO} \underset{k_{off(CO)}}{\overset{k_{on(CO)}}{\rightleftharpoons}} \text{Hp:Hb(II)-CO} + \text{NO}$$

Scheme 1. Reaction mechanism of Hp1–1:Hb(II)-NO and Hp2–2:Hb(II)-NO conversion to Hp:Hb1–1(II)-CO and Hp2–2:Hb(II)-CO, respectively.

M, respectively) were prepared by adding dithionite (final concentration 2.0×10^{-3} M) followed by the NO solution (final concentration 1.0×10^{-5} M) to the deoxygenated Hp1–1:Hb(II) and Hp2–2:Hb(II) solutions [30].

NO and CO were purchased from Aldrich Chemical Co. (Milwaukee, WI, USA) and Linde AG (Höllriegelskreuth, Germany), respectively. NO was purified by passing it through a glass column packed with NaOH pellets followed by passing it through a trapping solution, which contained 20 mL of 5.0 M NaOH, to remove traces impurities; the NO pressure was 760.0 mmHg [38]. The NO and CO solutions in 5.0×10^{-2} M phosphate buffer solution (pH = 7.2) were prepared in a closed vessel under NO or CO at P = 760.0 mmHg anaerobically at 20.0 °C. The solubility of NO and CO in the aqueous buffered solution was 2.05×10^{-3} M and 1.03×10^{-3} M, respectively, at P = 760.0 mmHg and 20.0 °C [15]. All the other chemicals, including D-*myo*-inositol 1,2,3,4,5,6-hexakisphosphate (IHP) and bezafibrate (BZF), were purchased from Merck AG (Darmstadt, Germany). All chemicals were of analytical or reagent grade and were used without further purification unless stated.

3. Methods

The values of the first-order rate constant for NO dissociation from Hp1–1:Hb(II)-NO and Hp2–2:Hb(II)-NO (*i.e.*, for NO replacement by CO; $k_{off(NO)}$) were determined by mixing the Hp1–1:Hb(II)-NO and Hp2–2:Hb(II)-NO (final concentration, 4.8×10^{-6} M and 4.6×10^{-6} M, respectively) solutions with the CO-dithionite solutions, in the absence and presence of IHP and BZF (final concentration, 2.0×10^{-2} M), under anaerobic conditions, at pH 7.0 (5.0×10^{-2} M phosphate buffer), and 20.0 °C; no gaseous phase was present [30]. Kinetics was carried out employing a SFM-20/MOS-200 rapid-mixing stopped-flow apparatus (BioLogic Science Instruments, Claix, France) and a Jasco V-650 spectrophotometer (Jasco, Tokyo, Japan), monitoring the progress curves at several single wavelengths spanning between 380 and 450 nm. The conversion of Hp1–1:Hb(II)-NO and Hp2–2:Hb(II)-NO to Hp1–1:Hb(II)-CO and Hp2–2:Hb(II)-CO, respectively, was fitted to a two-exponential process according to the minimum reaction mechanism represented by Scheme 1 [30]. The final CO concentration ranged between 2.0×10^{-4} M to 5.0×10^{-4} M and the final dithionite concentration was 2.0×10^{-3} M; the over 100-fold excess of CO over NO guarantees that the reaction proceeds rightward because $k_{on(CO)} \times [CO] >> k_{on(NO)} \times [NO]$ (see Scheme 1).

$$\text{Hp:Hb(II)-NO} + \text{CO} \underset{k_{on(NO)}}{\overset{k_{off(NO)}}{\rightleftharpoons}} \text{Hp:Hb(II)} + \text{NO} + \text{CO} \underset{k_{off(CO)}}{\overset{k_{on(CO)}}{\rightleftharpoons}} \text{Hp:Hb(II)-CO} + \text{NO}$$

The values of $k_{off(NO)1}$ and $k_{off(NO)2}$ have been determined from data analysis, according to two-exponential eq. (1):

$$A_t = A_1 \times e^{-koff(NO)1 \times t} + A_2 \times e^{-koff(NO)2 \times t} \quad (1)$$

where A_t refers to the relative signal amplitude at a given time = t for the reaction to be completed (*i.e.*, $[Hp:Hb(II)\text{-}NO]_t$ / $[Hp:Hb(II)]_{tot}$) and $A_1 + A_2 = 1$ (*i.e.*, 100% of the reaction) refers to the relative spectroscopic contribution of the two subunits, characterized by $k_{off(NO)1}$ and $k_{off(NO)2}$, respectively.

For comparison, kinetic data have also been analyzed according to the one-exponential eq. (2):

$$A_t = A \times e^{-koff(NO) \times t} \quad (2)$$

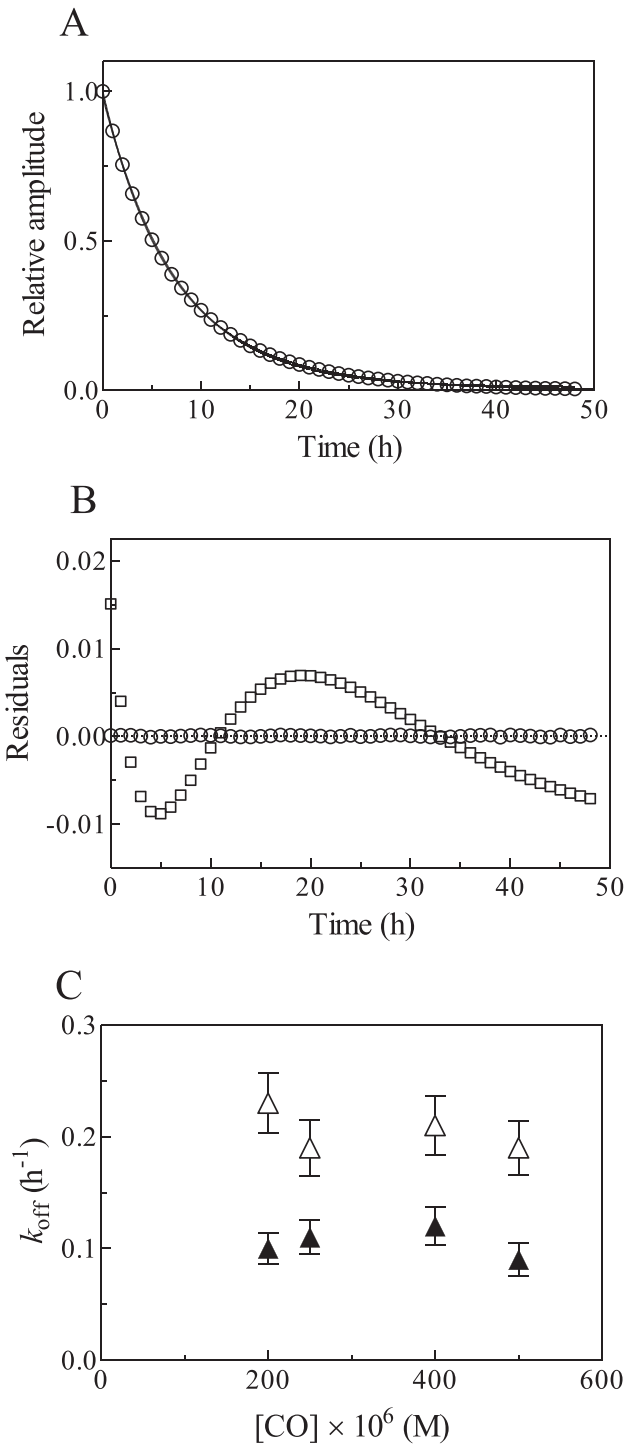

Fig. 2. Kinetics of NO dissociation from Hp2–2:Hb(II)-NO, at pH 7.0 and 20.0 °C. (A) Time course of NO dissociation from Hp2–2:Hb(II)-NO. The CO concentration was 5.0×10^{-4} M. The time course analysis according to eq. (1) allowed to determine the values of $k_{off\ (NO)1} = 1.9 \times 10^{-1}$ h^{-1} (= 5.3×10^{-5} s^{-1}), $A_1 = 0.51$, $k_{off\ (NO)2} = 9.0 \times 10^{-2}$ h^{-1} (= 2.5×10^{-5} s^{-1}). and $A_2 = 0.49$. The time course analysis according to eq. (2) allowed to determine the values of $k_{off\ (NO)} = 1.3 \times 10^{-1}$ h^{-1} (= 3.6×10^{-5} s^{-1}) and $A = 1.0$. (B) Residuals obtained from the non-linear least-squares fitting with one (squares; eq. (2)) and two (circles; eq. (1)) exponential(s) of data referring to NO dissociation from Hp2–2:Hb(II)-NO. (C) Dependence of the first order rate constant for NO dissociation from Hp2–2:Hb(II)-NO on the CO concentration. The average values of $k_{off\ (NO)1}$ and $k_{off(NO)2}$ are 2.1×10^{-1} h^{-1} (= 5.8×10^{-5} s^{-1}) and 1.1×10^{-1} h^{-1} (= 3.1×10^{-5} s^{-1}), respectively. The Hp1–1:Hb(II)-NO concentration was 4.6×10^{-6} M. The dithionite concentration was 2.0×10^{-3} M.

Table 1
Values of $k_{on(NO)}$ and $k_{off(NO)}$ for (de)nitrosylation of Hb(II)(-NO), Hp1–1:Hb(II)(-NO), Hp2–2:Hb(II)(-NO), α(II)(-NO), and β(II)(-NO) species.

Heme-protein	$k_{on(NO)}$ (M^{-1} s^{-1})	$k_{off(NO)}$ (s^{-1})	$k_{off1(NO)}$ (s^{-1})	$k_{off2(NO)}$ (s^{-1})
Hb(II)(-NO) + IHP (T-state)	2.5×10^7 [a]		3.1×10^{-3} [b] 1.1×10^{-3} [c]	9.0×10^{-5}[b] 4.2×10^{-4}[c]
Hb(II)(-NO) (R-state)	2.5×10^7 [a]	1.8×10^{-5}[b]		
Hp1–1:Hb(II)(-NO)	$(1.1 \pm 0.1) \times 10^7$ [d]		$(6.4 \pm 0.8) \times 10^{-5}$[e]	$(3.6 \pm 0.5) \times 10^{-5}$[e]
Hp1–1:Hb(II)(-NO) + IHP [e]			$(6.3 \pm 0.7) \times 10^{-5}$	$(3.1 \pm 0.4) \times 10^{-5}$
Hp1–1:Hb(II)(-NO) + BZF [e]			$(7.7 \pm 0.9) \times 10^{-5}$	$(2.9 \pm 0.5) \times 10^{-5}$
Hp2–2:Hb(II)(-NO)	$(9.3 \pm 0.9) \times 10^6$ [f]		$(5.8 \pm 0.8) \times 10^{-5}$ [e]	$(3.1 \pm 0.6) \times 10^{-5}$ [e]
Hp2–2:Hb(II)(-NO) + IHP [e]			$(6.3 \pm 0.7) \times 10^{-5}$	$(3.5 \pm 0.4) \times 10^{-5}$
Hp2–2:Hb(II)(-NO) + BZF [e]			$(6.9 \pm 0.8) \times 10^{-5}$	$(3.8 \pm 0.5) \times 10^{-5}$
α(II)(-NO) chains [a]	2.4×10^7	4.6×10^{-5}		
β(II)(-NO) chains [a]	2.4×10^7	2.2×10^{-5}		

[a] pH 7.0 and 20.0 °C. From [30].
[b] pH 7.0 and 20.0 °C. From [33].
[c] pH 7.4 and 20.0 °C. From [51]. The slower rate refers specifically to penta-coordinated α-chains of tetrameric Hb(II)-NO.
[d] pH 7.5 and 20.0 °C. From [21].
[e] pH 7.0 and 20.0 °C. Present study.
[f] pH 7.6 and 20.0 °C. From [21].

where $A = 1$.

The absorbance spectra of Hp1–1:Hb(II)-NO and Hp2–2:Hb(II)-NO were recorded between 380 and 450 nm in the absence and presence of IHP and BZF (final concentration, 2.0×10^{-2} M), at pH 7.0 (5.0×10^{-2} M phosphate buffer), and 20.0 °C [17,39,40]. Of note, IHP and BZF shift the quaternary equilibrium of tetrameric Hb(II)-NO from the hexacoordinated high affinity R-state to the penta-coordinated low affinity T-state. IHP- and BZF-mediated changes of the quaternary equilibrium of Hb(II)-NO can be easily detected by absorbance spectroscopy [17,39,40].

The results are given as mean values of at least four experiments plus or minus the corresponding standard deviation. All data were analyzed using the GraphPad Prism program, version 5.03 (GraphPad Software, La Jolla, CA, USA).

Molecular docking simulations were only carried out for IHP (RCSB PDB ligand ID: IHP) binding to Hb(II)-CO (PDB ID: 2DN3) [41] using the software DockingApp [42], a graphical interface for AutoDock Vina [43], limiting the grid box to the Hb(II)-CO:IHP interacting residues [44]. The IHP structure was retrieved from RCSB PDB (ligand ID: IHP) in sdf format. Subsequently it was first converted in pdb format, using The Open Babel Package version 2.4.1 [45], and then in pdbqt format through the MGLTools script "prepare_ligand4.py" [46]. The docking results for the Hb(II)-CO:IHP complex were analyzed by the molecular graphics software UCSF-Chimera version 1.13.1 [47]. Moreover, amino acid residues recognizing BZF bound to Hb(II)-O_2 (PDB ID: 5X2S and 5X2T) [48] were identified with the Protein-Ligand Interaction Profiler web server (https://projects.biotec.tu-dresden.de/plip-web/plip/index) [49].

4. Results and discussion

The NO dissociation reaction from Hp1–1:Hb(II)-NO and Hp2–2:Hb(II)-NO through displacement by CO (in the presence of dithionite) conforms to the minimum reaction mechanism depicted in Scheme 1. Of note, the rate of NO dissociation from Hp1–1:Hb(II)-NO and Hp2–2:Hb(II)-NO represents the rate limiting step of the whole process. Thus, upon

Table 2
Effect of IHP and BZF on values of λ_{max} and ε of the absorbance spectra of Hb(II)-NO, Hp1–1:Hb(II)-NO, and Hp2–2:Hb(II)-NO in the Soret region.

Heme-protein	λ_{max} (nm)	ε (mM^{-1} cm^{-1})
Hb(II)(-NO) + IHP (R-state)	417.0 [a]	133 [a]
	416.7 [b]	131 [b]
	417.2 [c]	131 [c]
Hb(II)(-NO) + IHP (T-state)	415.9 [a]	98 [a]
	415.2 [b]	99 [b]
	416.2 [c]	101.8 [c]
Hb(II)(-NO) + BZF (T-state)	416.9 [a]	101.3 [a]
	416.2 [c]	105.2 [c]
Hp1–1:Hb(II)(-NO) [a]	417.2	131
Hp1–1:Hb(II)(-NO) + IHP [a]	416.8	129
Hp1–1:Hb(II)(-NO) + BZF [a]	417.1	132
Hp2–2:Hb(II)(-NO) [a]	416.9	133
Hp2–2:Hb(II)(-NO) + IHP [a]	416.6	131
Hp2–2:Hb(II)(-NO) + BZF [a]	416.8	130

[a] pH 7.0 and 20.0 °C. Present study.
[b] pH 6.5 and 20.0 °C. From [39].
[c] pH 7.0 and 20.0 °C. From [40].

NO dissociation, Hp1–1:Hb(II) and Hp2–2:Hb(II) react much more rapidly with CO than with NO; in fact, $k_{on(CO)} \times$ [CO] ranges from 3.8×10^2 s^{-1} to 2.6×10^3 s^{-1} (*i.e.*, [CO] ranges from 2.0×10^{-4} M to 5.0×10^{-4} M and $k_{on(CO)} = 1.9 \times 10^6$ M^{-1} s^{-1} and 5.2×10^6 M^{-1} s^{-1} for Hp1–1:Hb(II) and Hp2–2:Hb(II), respectively) [11] whereas $k_{on(NO)} \times$ [NO] ranges from 4.5×10^1 s^{-1} to 5.5×10^1 s^{-1} (*i.e.*, [NO] = 5.0×10^{-6} M and $k_{on(NO)} = 1.1 \times 10^7$ M^{-1} s^{-1} and 9.3×10^6 M^{-1} s^{-1} for Hp1–1:Hb(II) and Hp2–2:Hb(II), respectively) [21], decreasing even further because of NO consumption by sodium dithionite [30,50], thus rendering even more reliable the determination of the NO dissociation rate constant.

Over the whole CO concentration range explored (final concentration, 2.0×10^{-4} M to 5.0×10^{-4} M), the time course of Hp1–1:Hb(II)-NO and Hp2–2:Hb(II)-NO conversion to Hp1–1:Hb(II)-CO and Hp2–2:Hb(II)-CO, respectively, by CO (in the presence of dithionite) corresponds to a bi-exponential process, the amplitude of both phases ranges from 47 ± 5% to 52 ± 5% of the total amplitude (Figs. 1 and 2, panel A, and Fig. 2 SM and 3 SM of Supplementary Material). Values of the first-order rate constants for Hp1–1:Hb(II)-NO and Hp2–2:Hb(II)-NO denitrosylation (*i.e.*, for Hp1–1:Hb(II)-CO and Hp2–2:Hb(II)-CO formation; $k_{off(NO)}$) are wavelength- and [CO]-independent.

The values of the fast and slow phase of NO dissociation from Hp1–1:Hb(II)-NO, Hp2–2:Hb(II)-NO (*i.e.*, $k_{off(NO)1}$ and $k_{off(NO)2}$, respectively) (present study): (*i*) are unaffected by IHP and BZF (Table 1), (*ii*) correspond to those of isolated α(II)-NO and β(II)-NO chains, respectively, (*iii*) match with those of NO dissociation from the R-state of Hb(II)-NO, and (*iv*) differ from those for the denitrosylation of the T-state of Hb(II)-NO [30,33,51] (Table 1). In both Hp:Hb(II)-NO complexes no evidence can be detected of the penta-coordinate nitrosylated α-chain, which is known to have a NO dissociation rate constant faster than in the R-state [30,33,51] and a low absorbance in the Soret region [17,39,40]. This is not unexpected, since in the Hp:Hb complexes dimers are in the R quaternary conformation, while penta-coordination seems associated to the low affinity T-structure [30,33,51].

On the other hand, it is known that also in the R-state tetrameric Hb is able to bind allosteric effectors, such as inositol hexakisphosphate (IHP) and bezafibrate (BZF), displaying both functional [52,53] and spectroscopic effects [17,39,40], envisaging structural arrangement of both subunits [40,52–54]. However, in the case of Hp:Hb complexes neither functional nor spectroscopic effects appear associated to the addition of either IHP or BZF (Tables 1 and 2), envisaging the possibility that either they do not bind the dimer associated to Hp or else they do not affect the structural arrangement of the dimers in the Hp:Hb complexes.

The molecular bases of a lack of effect of IHP and BZF on NO

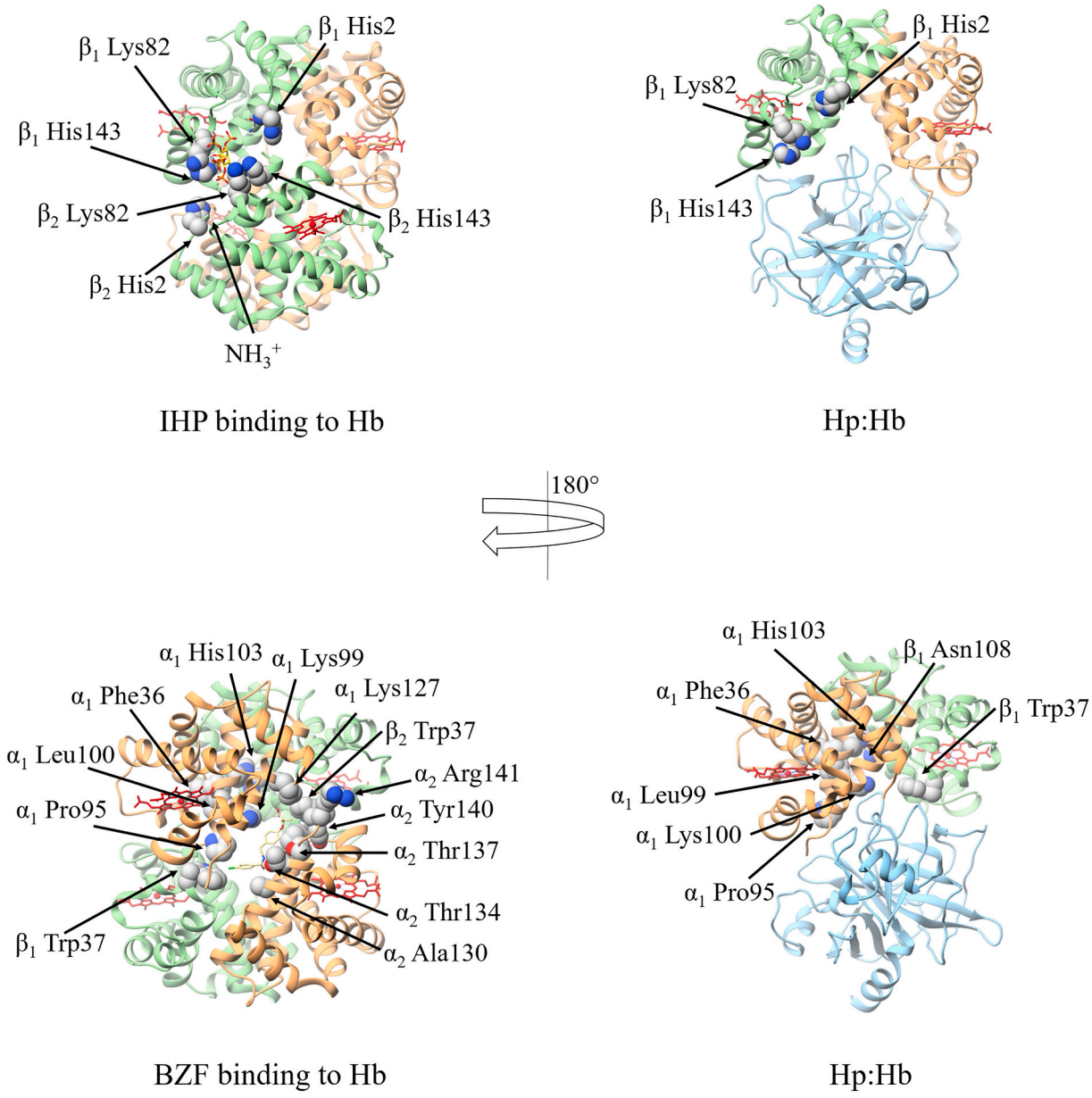

Fig. 3. Amino acid residues involved in IHP and BZF binding to tetrameric ligated Hb(II) are solvent-exposed or participate in Hp1–1:Hb(II)-O_2 complexation. The α and β chains of Hb are in orange and green, respectively, and the heme groups are in red. The serine proteinase-like domain of Hp is in light blue. Amino acid residues of ligated Hb(II) involved in IHP and BZF are in gray. The pictures have been drawn with UCSF-Chimera [47]. (For interpretation of the references to colour in this figure legend, the reader is referred to the web version of this article.)

dissociation from Hp1–1:Hb(II)-NO, Hp2–2:Hb(II)-NO and on the absorbance spectroscopic properties of Hp1–1:Hb(II)-NO, Hp2–2:Hb(II)-NO have been investigated through molecular docking analyses. IHP binding to tetrameric Hb involves the β_1 *N*-terminus, β_1 and β_2 His2, β_1 and β_2 Lys82, and β_1 and β_2 His143 [44]. The results of molecular docking simulations do not evidence binding of IHP in the vicinity of the above mentioned residues (Fig. 3). Although the β_1 *N*-terminus, β_1 His2, β_1 Lys82, and β_1 His143 are solvent exposed in the Hp:Hb complex, the absence of IHP binding to the Hp:Hb complex may reflect the disruption of the IHP cleft that is built up by both the $\alpha_1\beta_1$ and $\alpha_2\beta_2$ dimers in tetrameric Hb. In the case of BZF binding to tetrameric Hb (Fig. 3), the situation is more complex, since multiple ligand binding have been reported [48,55,56]. In fact, BZF is able to bind one β and two α subunits of Hb(II)-O_2 [48,55] interacting with the amino acids residues β_2 Trp37, α_1 Lys127, α_1 and α_2 Pro95 and α_2 Tyr140, at pH 6.5 (PDB ID: 5X2S) [48] and with β_1 Trp37, α_1 Lys127, α_2 Ala130 and α_2 Thr134, at pH 7.2 (PDB ID: 5X2T) [48] (Fig. 3). Thus, the loss of ability of the Hp:Hb complexes to bind BZF may reflect: (*i*) the involvement of residues α_1 Phe36, α_1 Pro95, α_1 Lys99, α_1 Leu100, α_1 His103, β_1 Trp37, and β_1 Asn108 in the Hp1–1:Hb(II)-O_2 complexation [8] and (*ii*) residues β_2 Trp37, α_2 Pro95, α_2 Ala130, α_2 Thr134, α_2 Thr137, α_2 Tyr140, and α_2 Arg141 do not participate to BZF recognition in tetrameric Hb [48] (Fig. 3). Since BZF interacts with the *E*-helix of the α-subunit in the tetrameric R-state of Hb (II)-CO [56], it cannot be excluded that BZF could recognize the Hp:Hb complexes in a similar fashion without affecting the reactivity and the absorbance spectroscopic properties of Hp:Hb complexes (Tables 1 and 2).

A closer view of the biphasic dissociation rate constants casts some light on the different free energy barriers between the α and β subunits for the NO detachment from the nitrosylated heme-Fe(II) atom and for the ligand exit pathway. In the fully NO-bound Hb the energy barrier for NO dissociation from α-chain (*i.e.*, 96.9 kJ/mol) is about 1.8 kJ/mol

Table 3
Values of kinetic and thermodynamic parameters for CO, O_2 and NO dissociation from ligated Hb(II) species.

Heme-protein	Ligand	k_{off} (s^{-1})	k_{off1} (s^{-1})	k_{off2} (s^{-1})	$\Delta G^{\ddagger}$ (kJ/mol)[a]	$\Delta G_1^{\ddagger}$ (kJ/mol) [a]	$\Delta G_2^{\ddagger}$ (kJ/mol) [a]
Hb(II) T-state [b]	CO	~ 0.2			76.6		
Hb(II) R-state [c]	CO		(1.1 ± 0.2) × 10^{-2}	(8.0 ± 0.2) × 10^{-3}		83.6 ± 0.5	84.4 ± 0.3
Hp1–1: Hb(II) [d]	CO		(1.4 ± 0.2) × 10^{-2}	(6.2 ± 0.8) × 10^{-3}		83.0 ± 0.3	85.0 ± 0.4
Hp2–2: Hb(II) [d]	CO		(1.3 ± 0.2) × 10^{-2}	(7.3 ± 0.9) × 10^{-3}		83.2 ± 0.3	84.6 ± 0.4
α(II) chains [b]	CO	1.3 × 10^{-2}			83.2		
β(II) chains [b]	CO	8.0 × 10^{-3}			84.4		
Hb(II) T-state [e]	O_2		(2.5 ± 0.1) × 10^{3}	(1.8 ± 0.1) × 10^{2}		53.7 ± 0.2	60.0 ± 0.3
Hb(II) R-state [c]	O_2		(4.0 ± 0.8) × 10^{1}	(1.2 ± 0.2) × 10^{1}		63.7 ± 0.5	66.6 ± 0.5
Hp1–1: Hb(II) [f]	O_2		(2.8 ± 0.3) × 10^{1}	(1.6 ± 0.2) × 10^{1}		64.6 ± 0.3	65.9 ± 0.3
Hp2–2: Hb(II) [f]	O_2		(2.7 ± 0.3) × 10^{1}	(1.4 ± 0.2) × 10^{1}		64.7 ± 0.3	66.2 ± 0.4
α(II) chains [b]	O_2	2.8 × 10^{1}			64.6		
β(II) chains [b]	O_2	1.6 × 10^{1}			65.9		
Hb(II) (T-state)	NO		3.1 × 10^{-3} [g] [h]1.1 × 10^{-3}	9.0 × 10^{-5} [g] 4.2 × 10^{-4}[h]		89.4 89.2	95.3 91.5
Hb(II) R-state [g]	NO	1.8 × 10^{-5}			99.2		
Hp1–1: Hb(II) [i]	NO		(6.4 ± 0.8) × 10^{-5}	(3.6 ± 0.5) × 10^{-5}		96.1 ± 0.3	97.5 ± 0.4
Hp2–2: Hb(II) [i]	NO		(5.8 ± 0.8) × 10^{-5}	(3.1 ± 0.6) × 10^{-5}		96.3 ± 0.3	97.9 ± 0.5
α(II) chains [j]	NO	4.6 × 10^{-5}			96.9		
β(II) chains [j]	NO	2.2 × 10^{-5}			98.7		

Footnote to Table 3.
[a] Values of $\Delta G^{\ddagger}$ have been calculated according to the following equation: $\Delta G^{\ddagger} = 4.184 \times R \times T\ (\ln(10^{13}) - \ln k)$.
[b] pH 7.0 and 20.0 °C. From [15].
[c] pH 7.4 and 25.0 °C. From [34].
[d] pH 7.0 and 20.0 °C. From [27].
[e] pH 7.0 and 20.0 °C. From [32].
[f] pH 7.0 and 20.0 °C. From [23].
[g] pH 7.0 and 20.0 °C. From [33].
[h] pH 7.4 and 20.0 °C. From [51]. The slower rate refers specifically to penta-coordinated α-chains of tetrameric Hb(II)-NO.
[i] pH 7.0 and 20.0 °C. Present study.
[j] pH 7.0 and 20.0 °C. From [30].

lower than for β-chain denitrosylation (*i.e.*, 98.7 kJ/mol). Of note, this difference (*i*) can be observed between the two subunits within the Hb dimer both in Hp1–1:Hb(II)-NO ($\Delta\Delta G^{\ddagger} = 1.4$ kJ/mol) and Hp2–2:Hb(II)-NO ($\Delta\Delta G^{\ddagger} = 1.6$ kJ/mol), and (*ii*) is similar to that observed in other ligands of the ferrous form (*i.e.*, CO and O_2), displaying a ligand-independent value of $\Delta\Delta G^{\ddagger} = 1.5 \pm 0.3$ kJ/mol (see Table 3).

The closely similar difference between the two subunits for free energy barriers of CO, O_2 and NO dissociation from R-state ligated Hb(II) (see Table 3) clearly indicates that the kinetic biphasicity has the same structural basis, even though various ligands are characterized by markedly different energy barriers. As a whole, we can state that the free energy barriers for the ligand dissociation from the ligand-bound heme (II) complexes and exit toward the bulk solvent are different for the two subunits in R-state ligated Hb(II) by 1.6 ± 0.4 kJ/mol (Table 3); this ligand-independent value refers to the different structural arrangement of the two subunits for any ligand exit pathway after the breaking of the Fe(II)-ligand bond.

On the other hand, the intrinsic values of $\Delta G^{\ddagger}$ greatly differ for various ligands (see Table 3), this reflecting instead the specific ligand-dependent interactions of each ligand with the distal site of the protein matrix in the R quaternary conformation. In this respect, data reported in Table 3 give an exhaustive description of the intrinsic subunit functional heterogeneity also in assembled dimers, clearly demonstrating that in assembled $\alpha_1\beta_1$ (as well as in $\alpha_2\beta_2$) dimers the structural arrangement of the two subunits does not show meaningful differences from isolated chains and/or tetramers (see Table 1 and [23,27]). However, the origin of the different ligand-dependent quaternary-linked effect remains elusive. In conclusion, unlike for O_2 and CO [32,34,55,57,58], the time-course for NO association to Hb(II) does not reflect the R-to-T allosteric transition [30], the cooperativity of Hb(II) nitrosylation depending uniquely on the ligand dissociation process. In fact, values of k_{off} for NO dissociation from the T- and R-state of Hb(II) differ by 2-orders of magnitude while the association rate constants are essentially identical for the two quaternary conformations (see Table 1). This strongly suggests that determinants for the different ligand-dependent quaternary-linked effects on ligand binding are multifactorial, underlying a much more complex regulatory mechanism.

Declaration of Competing Interest

The authors declare no conflict of interest.

Acknowledgments

Authors wish to thank Prof. Fabio Polticelli for critical reading of the manuscript. The grant of Dipartimenti di Eccellenza, MIUR (Legge 232/2016, Articolo 1, Comma 314-337) is gratefully acknowledged.

Appendix A. Supplementary data

Supplementary data to this article can be found online at https://doi.org/10.1016/j.jinorgbio.2020.111272.

References

[1] M. Kristiansen, J.H. Graversen, C. Jacobsen, O. Sonne, H.J. Hoffman, K. Law, S. K. Moestrup, Nature 409 (2001) 198–201.
[2] P.W. Buehler, B. Abraham, F. Vallelian, C. Linnemayr, C.P. Pereira, J.F. Cipollo, Y. Jia, M. Mikolajczyk, F.S. Boretti, G. Schoedon, A.I. Alayash, D.J. Schaer, Blood 113 (2009) 2578–2586.
[3] T. Kaempfer, E. Duerst, P. Gehrig, B. Roschitzki, D. Rutishauser, J. Grossmann, G. Schoedon, F. Vallelian, D.J. Schaer, J. Proteome, Res. 10 (2011) 2397–2408.
[4] J.H. Baek, F. D'Agnillo, F. Vallelian, C.P. Pereira, M.C. Williams, Y. Jia, D.J. Schaer, P.W. Buehler, J. Clin. Invest. 122 (2012) 1444–1458.
[5] A.I. Alayash, C.B. Andersen, S.K. Moestrup, L. Bülow, Trends Biotechnol. 31 (2013) 2–3.
[6] T.L. Mollan, Y. Jia, S. Banerjee, G. Wu, R.T. Kreulen, A.L. Tsai, J.S. Olson, A. L. Crumbliss, A.I. Alayash, Free Radic. Biol. Med. 69 (2014) 265–277.

[7] C.B.F. Andersen, K. Stødkilde, K.L. Sæderup, A. Kuhlee, S. Raunser, J.H. Graversen, S.K. Moestrup, Antioxid. Redox Signal. 26 (2017) 814–831.
[8] A. di Masi, G. De Simone, C. Ciaccio, S. D'Orso, M. Coletta, P. Ascenzi, Mol. Asp. Med. 73 (2020) 100851.
[9] C.B.F. Andersen, M. Torvund-Jensen, M.J. Nielsen, C.L. de Oliveira, H.P. Hersleth, N.H. Andersen, J.S. Pedersen, G.R. Andersen, S.K. Moestrup, Nature 489 (2012) 456–459.
[10] R.L. Nagel, J.B. Wittenberg, H.M. Ranney, Biochim. Biophys. Acta 100 (1965) 286–289.
[11] R.L. Nagel, Q.H. Gibson, J. Mol, Biol. 22 (1966) 249–255.
[12] M. Brunori, A. Alfsen, U. Saggese, E. Antonini, J. Wyman, J. Biol. Chem. 243 (1968) 2950–2954.
[13] Q.H. Gibson, L.J. Parkhurst, G. Geraci, J. Biol. Chem. 244 (1969) 4668–4676.
[14] E. Alfsen, E. Chiancone, E. Antonini, M. Waks, J. Wyman, Biochim. Biophys. Acta 207 (1970) 395–403.
[15] E. Antonini, M. Brunori, Hemoglobin and Myoglobin in their Reactions with Ligands, North Holland Publishing Co, Amsterdam, London, 1971.
[16] E. Chiancone, E. Antonini, M. Brunori, A. Alfsen, F. Lavialle, Biochem. J. 133 (1973) 205–207.
[17] M.F. Perutz, Annu. Rev. Biochem. 48 (1979) 327–386.
[18] A. Kurosky, D.R. Barnett, T.H. Lee, B. Touchstone, R.E. Hay, M.S. Arnott, B. H. Bowman, W.M. Fitch, Proc. Natl. Acad. Sci. U. S. A. 77 (1980) 3388–3392.
[19] I. Azarov, X. He, A. Jeffers, S. Basu, B. Ucer, R.R. Hantgan, A. Levy, D.B. Kim-Shapiro, Nitric Oxide 18 (2008) 296–302.
[20] P. Ascenzi, M. Coletta, J. Phys, Chem. B 122 (2018) 11100–11107.
[21] P. Ascenzi, G. De Simone, F. Polticelli, M. Gioia, M. Coletta, J, Biol, Inorg. Chem. 23 (2018) 437–445.
[22] P. Ascenzi, G.R. Tundo, M. Coletta, J. Inorg. Biochem. 187 (2018) 116–122.
[23] P. Ascenzi, F. Polticelli, M. Coletta, Sci. Rep. 9 (2019) 6780.
[24] S.L. White, J. Biol. Chem. 250 (1975) 1263–1268.
[25] P. Ascenzi, A. di Masi, G. De Simone, M. Gioia, M. Coletta, J. Biol. Inorg. Chem. 24 (2019) 247–255.
[26] P. Ascenzi, G. De Simone, C. Ciaccio, M. Coletta, J. Inorg. Biochem. 202 (2020) 110814.
[27] P. Ascenzi, G. De Simone, G.R. Tundo, M. Coletta, J. Biol. Inorg. Chem. 25 (2020) 351–360.
[28] M. Coletta, M. Angeletti, G. De Sanctis, L. Cerroni, B. Giardina, G. Amiconi, P. Ascenzi, Eur. J. Biochem. 235 (1996) 49–53.
[29] M. Hoshino, M. Maeda, R. Konishi, H. Seki, P.C. Ford, J. Am. Chem. Soc. 118 (1996) 5702–5707.
[30] E.G. Moore, Q.H. Gibson, J. Biol. Chem. 251 (1976) 2788–2794.
[31] P. Ascenzi, A. di Masi, F. Gullotta, M. Mattu, C. Ciaccio, M. Coletta, Biochem. Biophys. Res. Commun. 393 (2010) 196–200.
[32] C.A. Sawicki, Q.H. Gibson, J. Biol. Chem. 252 (1977) 7538–7547.
[33] V.S. Sharma, H.M. Ranney, J. Biol. Chem. 253 (1978) 6467–6472.
[34] K.D. Vandegriff, Y.C. Le Tellier, R.M. Winslow, R.J. Rohlfs, J.S. Olson, J. Biol. Chem. 266 (1991) 17049–17059.
[35] C.Y. Liau, K.C. Uengb, C.S. Lin, J. Chin, Chem. Soc-Taip 56 (2009) 859–866.
[36] Y. Jia, F. Wood, P.W. Buehler, A.I. .Alayash, PLoS One 8 (2013) e59841.
[37] C.E. Allen, M.P. Schmitt, J. Bacteriol. 197 (2015) 553–562.
[38] R.M. Barbosa, A.J. Lopes Jesus, R.M. Santos, C.L. Pereira, C.F. Marques, B.S. Rocha, N.R. Ferreira, A. Ledo, J. Laranjin, Global J. Anal. Chem. 2 (2011) 272–284.
[39] M.F. Perutz, J.V. Kilmartin, K. Nagai, A. Szabo, S.R. Simon, Biochemistry 15 (1976) 378–387.
[40] P. Ascenzi, A. Bertollini, M. Coletta, A. Desideri, B. Giardina, F. Polizio, R. Santucci, R. Scatena, G. Amiconi, J. Inorg. Biochem. 50 (1993) 263–272.
[41] S.-Y. Park, T. Yokoyama, N. Shibayama, Y. Shiro, J.R.H. Tame, J. Mol. Biol. 360 (2006) 690–701.
[42] E. Di Muzio, D. Toti, F. Polticelli, J. Comput, Aided Mol. Des. 31 (2017) 213–218.
[43] O. Trott, A.J. Olson, J. Comput. Chem. 31 (2010) 455–461.
[44] A. Arnone, M.F. Perutz, Nature 249 (1974) 34–36.
[45] N.M. O'Boyle, M. Banck, C.A. James, C. Morley, T. Vandermeersch, G. R. Hutchison, J. Cheminf. 3 (2011) 33.
[46] G. Morris, R.J. Huey, Comput. Chem. 30 (2009) 2785–2791.
[47] E.F. Pettersen, T.D. Goddard, C.C. Huang, G.S. Couch, D.M. Greenblatt, E.C. Meng, T.E. Ferrin, J. Comput. Chem. 25 (2004) 1605–1612.
[48] N. Shibayama, M. Ohki, J. R. H. Tame, Park S.-Y. J. Biol. Chem. 292 (2017) 18258–18269.
[49] S. Salentin, S. Schreiber, V.J. Haupt, M.F. Adasme, M. Schroeder, Nucl Acids Res. 43 (2015) W443–W447.
[50] R. Grubina, S. Basu, M. Tiso, D.B. Kim-Shapiro, M.T. Gladwin, J. Biol. Chem. 283 (2008) 3628–3638.
[51] F. Azizi, J.E. Kielbasa, A.M. Adeyiga, R.D. Maree, M. Frazier, M. Yakubu, H. Shields, S.B. King, D.B. Kim-Shapiro, Free Rad. Biol. & Med. 39 (2005) 145–151.
[52] M. Coletta, P. Ascenzi, R. Santucci, A. Bertollini, G. Amiconi, Biochim. Biophys. Acta 1162 (1993) 309–314.
[53] M. Coletta, P. Ascenzi, M. Castagnola, B. Giardina, J. Mol. Biol. 249 (1995) 800–803.
[54] G. De Sanctis, A.M. Priori, F. Polizio, P. Ascenzi, M. Coletta, J. Biol. Inorg. Chem. 3 (1998) 135–139.
[55] M.F. Perutz, G. Fermi, D.J. Abraham, C. Poyart, E. Bursaux, J. Am. Chem. Soc. 108 (1986) 1064–1078.
[56] N. Shibayama, S. Miura, J.R.H. Tame, T. Yonetani, S.-Y. Park, J. Biol. Chem. 277 (2002) 38791–38796.
[57] P. Reisberg, J.S. Olson, J. Biol. Chem. 256 (1980) 4159–4169.
[58] M. Perrella, N. Davids, L. Rossi-Bernardi, J. Biol. Chem. 267 (1992) 8744–8751.